

This article appeared in a journal published by Elsevier. The attached copy is furnished to the author for internal non-commercial research and education use, including for instruction at the authors institution and sharing with colleagues.

Other uses, including reproduction and distribution, or selling or licensing copies, or posting to personal, institutional or third party websites are prohibited.

In most cases authors are permitted to post their version of the article (e.g. in Word or Tex form) to their personal website or institutional repository. Authors requiring further information regarding Elsevier's archiving and manuscript policies are encouraged to visit:

<http://www.elsevier.com/copyright>



Contents lists available at ScienceDirect

Analytical Biochemistry

journal homepage: www.elsevier.com/locate/yabio

Use of thermal melt curves to assess the quality of enzyme preparations

Gregory J. Crowther^{a,*}, Panqing He^a, Philip P. Rodenbough^a, Andrew P. Thomas^a, Kuzma V. Kovzun^a, David J. Leibly^a, Janhavi Bhandari^a, Lisa J. Castaneda^a, Wim G.J. Hol^b, Michael H. Gelb^{b,c}, Alberto J. Napuli^b, Wesley C. Van Voorhis^{a,*}

^a Department of Medicine, University of Washington, Seattle, WA 98195, USA

^b Department of Biochemistry, University of Washington, Seattle, WA 98195, USA

^c Department of Chemistry, University of Washington, Seattle, WA 98195, USA

ARTICLE INFO

Article history:

Received 26 October 2009

Received in revised form 5 December 2009

Accepted 9 December 2009

Available online 14 December 2009

Keywords:

Thermal melting

Malaria

Protein denaturation

ABSTRACT

This study sought to determine whether the quality of enzyme preparations can be determined from their melting curves, which may easily be obtained using a fluorescent probe and a standard reverse transcription-polymerase chain reaction (RT-PCR) machine. Thermal melt data on 31 recombinant enzymes from *Plasmodium* parasites were acquired by incrementally heating them to 90 °C and measuring unfolding with a fluorescent dye. Activity assays specific to each enzyme were also performed. Four of the enzymes were denatured to varying degrees with heat and sodium dodecyl sulfate (SDS) prior to the thermal melt and activity assays. In general, melting curve quality was correlated with enzyme activity; enzymes with high-quality curves were found almost uniformly to be active, whereas those with lower quality curves were more varied in their catalytic performance. Inspection of melting curves of bovine xanthine oxidase and *Entamoeba histolytica* cysteine protease 1 allowed active stocks to be distinguished from inactive stocks, implying that a relationship between melting curve quality and activity persists over a wide range of experimental conditions and species. Our data suggest that melting curves can help to distinguish properly folded proteins from denatured ones and, therefore, may be useful in selecting stocks for further study and in optimizing purification procedures for specific proteins.

© 2009 Elsevier Inc. All rights reserved.

Thorough characterization of a purified protein requires that it be in its naturally folded (native) state. Functional assays such as enzyme activity assays can indicate whether or not a protein is well-folded; however, for any given protein, an assay might not exist or may require expensive ingredients, extensive sample processing, and/or complex instrumentation. Moreover, as numerous organisms undergo genome-wide characterization, there will be increasing interest in previously obscure (and therefore difficult-to-assay) proteins, including those whose functions are not yet known.

Given the limitations of functional assays as indicators of protein folding, an alternative method for assessing folding status could be quite useful. Thermal melting with fluorescent dye that binds to a protein's exposed hydrophobic regions [1] might be such a method; a large heat-induced increase in fluorescence suggests that the protein was well-folded prior to heating [2]. To our knowledge, however, it is not yet clear whether, among a variety of proteins, melting curve properties can be correlated with an independent readout of folding status.

In the current study, stocks of more than 30 enzymes, mostly from *Plasmodium* parasites that cause malaria, were characterized via thermal melt and activity assays. Our goal was to determine whether enzymes' melting curves are predictive of activity, with the latter being a proxy for folding state. Our results suggest that melting curves are indeed a convenient indicator of whether enzymes, and presumably other proteins, are properly folded.

Materials and methods

Enzyme sources, production, and purification

Recombinant histidine-tagged enzymes from *Plasmodium berghei*, *P. falciparum*, *P. knowlesi*, and *P. vivax* were expressed in *Escherichia coli* and purified by immobilized metal affinity chromatography essentially as described previously [3]. Guanosine 5'-triphosphate (GTP)¹ cyclohydrolase from *E. coli* [4] was obtained in a

* Corresponding authors. Fax: +1 206 685 8681 (G.J. Crowther), +1 206 616 4898 (W.C. Van Voorhis).

E-mail addresses: crowther@uw.edu (G.J. Crowther), wesley@uw.edu (W.C. Van Voorhis).

¹ Abbreviations used: GTP, guanosine 5'-triphosphate; ATP, adenosine 5'-triphosphate; AMC, 7-amino-4-methyl coumarin; DTT, dithiothreitol; EDTA, ethylenediaminetetraacetic acid; TDP, thymidine 5'-diphosphate; UDP, uridine 5'-diphosphate; GRAVY, grand average of hydropathy; SDS, sodium dodecyl sulfate; ITD, isothermal denaturation; DLS, differential static light scattering; CD, circular dichroism.

similar manner, whereas procedures for purification and refolding of cysteine protease 1 from *Entamoeba histolytica* were based on those of a previous study [5]. Xanthine oxidase from *Bos taurus* and other non-*Plasmodium* enzymes used in coupled activity assays (glucose-6-phosphate dehydrogenase, lactate dehydrogenase, phosphoglucate dehydrogenase, pyrophosphatase, and pyruvate kinase) were purchased from Sigma–Aldrich (St. Louis, MO, USA).

Acquisition and quantitation of thermal melt data

Melting curves of enzyme stocks were obtained from samples in 96-well plates using a DNA Engine Opticon 2 (manufactured by MJ Research, now part of Bio-Rad) and the fluorescent probe SYPRO Orange (Invitrogen, Carlsbad, CA, USA) as described previously [3]. In brief, a heating rate of approximately 1.2 °C/min was used, and fluorescence readings (excitation at 530 ± 30 nm, emission at 575 ± 20 nm) were taken after each 0.2° increase. *Plasmodium* enzymes were diluted both in a standard thermal melt buffer (100 mM Hepes and 150 mM NaCl, pH 7.5) and in the enzyme-specific activity assay buffers listed in Table 1. Xanthine oxidase from *B. taurus* was heated in the buffers also used for superoxide dismutase, whereas cysteine protease 1 from *E. histolytica* was heated in a buffer of 20 mM Tris, 250 mM NaCl, 5% glycerol, and 125 mM L-arginine (pH 8.0). Each melting curve was assigned a quality score (Q) calculated as $Q = \Delta F_{\text{melt}} / \Delta F_{\text{total}}$, where ΔF_{melt} is the melting-associated increase in fluorescence and ΔF_{total} is the total range in fluorescence observed between 20 and 90 °C (i.e., the difference between the minimum and maximum values recorded over the 20–90° span). The range of possible Q values is 0–1, with 0 designating an absence of discernible melting behavior and 1 representing a high-quality melting curve.

Activity assays

All activity assays were done at room temperature (20–25 °C). Instruments used included a BioSpec-1601 spectrophotometer made by Shimadzu (Kyoto, Japan) and ELx800 and FLx800 microplate readers made by BioTek Instruments (Winooski, VT, USA). Whenever possible, enzymes were assayed according to precedents in the literature (see Refs. in Table 1) using substrate concentrations well above the corresponding K_m values. Enzymes were assayed in the direction corresponding to their names (e.g., with glutamate dehydrogenase, we measured the formation of NADPH corresponding to the dehydrogenation of glutamate, not the consumption of NADPH by the hydrogenation of 2-oxoglutarate) unless specified otherwise. The high bovine serum albumin concentrations (0.5–1.25 mg/ml) used in previous activity assays of choline kinase [6] and dUTPase [7] were omitted from our thermal melt and activity assays because they interfere with the fluorescent readout of the thermal melt assay. Other exceptions and clarifications are as follows.

6-Phosphogluconolactonase. A previous report on the *P. berghei* enzyme [8] did not specify the assay buffer used. The buffer listed in Table 1 was taken from a reference cited by that report [9].

6-Pyruvoyltetrahydropterin synthase. Activity was confirmed via a coupled assay in which 7,8-dihydroneopterin triphosphate, the substrate of 6-pyruvoyltetrahydropterin synthase, was generated from GTP by recombinant GTP cyclohydrolase from *E. coli*. A time-dependent increase in fluorescence (excitation at 360 nm, emission at 460 nm) beyond that seen with GTP and GTP cyclohydrolase alone was observed when 6-pyruvoyltetrahydropterin synthase was added, and the extent of the increase above the baseline rate was proportional to the concentration of 6-pyruvoyltetrahydropterin synthase.

Choline kinase. Choline-dependent adenosine 5'-triphosphate (ATP) consumption was measured with Kinase-Glo [10].

Cysteine protease 1. Measurement of the release of fluorescent 7-amino-4-methyl coumarin (AMC) from the substrate Z-Arg-Arg-AMC was based on a previous report [11]. The buffer used was 100 mM citric acid–NaHPO₄, 5 mM dithiothreitol (DTT), and 2 mM ethylenediaminetetraacetic acid (EDTA) (pH 6.0).

Dihydrofolate synthase. The dihydropteroate-dependent production of inorganic phosphate was measured with malachite green [12].

dUTPase and farnesyl pyrophosphate synthase. Pyrophosphatase from *Saccharomyces cerevisiae* was used to cleave pyrophosphate (a product of both enzymes) into inorganic phosphate, which was detected with malachite green [12].

Glycerol-3-phosphate dehydrogenase. The reaction was studied in the NADH-consuming direction.

Guanylate kinase. The previously published activity assay protocol [13] suggested a buffer that includes 0.5 mM EDTA and 5.7 mM MgSO₄, whereas the current study used no EDTA and 2 mM MgCl₂.

Hydroxymethyl-dihydropterin pyrophosphokinase. Hydroxymethyl-dihydropterin-dependent ATP consumption was measured with Kinase-Glo [10].

Methionine adenosyltransferase. Production of inorganic phosphate was measured with malachite green [12].

Methionine aminopeptidase 1. A previous characterization of the *Plasmodium* enzyme used a dipeptide substrate [14], whereas the current study used L-methionine-p-nitroanilide as the substrate [15].

N-Myristoyltransferase. The peptide substrate used was GSSYSRKNK, which was based on the N-terminal sequence of adenylylate kinase 2, a substrate of the *P. falciparum* N-myristoyltransferase in vivo [16]. Production of coenzyme A was measured with ThioGlo [17], which fluoresces (excitation at 379 nm, emission at 513 nm) on reacting with free sulfhydryl groups.

Nucleoside diphosphate kinase. A previous study of the *Plasmodium* enzyme used thymidine 5'-diphosphate (TDP) and ATP as substrates, whereas the current study used uridine 5'-diphosphate (UDP) and ATP. Activity was quantified as the rate of UDP-dependent ATP consumption as measured with Kinase-Glo [10].

Phosphoethanolamine N-methyltransferase. Production of S-adenosylhomocysteine was detected via the coupling enzymes S-adenosylhomocysteine hydrolase (which converts S-adenosylhomocysteine to homocysteine and adenosine) and adenosine deaminase (which converts adenosine to inosine). The concentration of S-adenosylhomocysteine produced was calculated from the slope of the decrease in absorbance at 267 nm representing conversion of adenosine to inosine based on a standard curve of ΔA_{267} versus [S-adenosylhomocysteine].

Phosphoglycerate kinase. Phosphoglycerate-dependent ATP consumption was measured with Kinase-Glo [10].

Superoxide dismutase. A previous study of the *Plasmodium* enzyme measured inhibition of the autooxidation of pyrogallol [18], whereas the current study measured inhibition of the reduction of cytochrome c [19].

Xanthine oxidase. Reduction of cytochrome c was tracked as described in the protocol for superoxide dismutase using the buffer described therein [19].

Preassay denaturation of four representative enzymes

Adenosine deaminase (from *P. vivax*), glyceraldehyde-3-phosphate dehydrogenase, methionine aminopeptidase 1, and orotidine 5'-monophosphate decarboxylase were studied at various levels of denaturation by subjecting them to heating and the detergent sodium dodecyl sulfate (SDS) prior to thermal melt and activity assays. These enzymes were chosen because they cover a range of chemical reactions (oxidoreductase, hydrolase, and lyase corresponding to EC groups 1, 3, and 4), numbers of subunits (monomer, dimer, and tetramer), and grand averages of hydropathy (GRAVY values: −0.045 to −0.482). The specific conditions (temperature

Table 1
Plasmodium enzymes studied by thermal melt and activity assays.

| Enzyme ^a | Gene ID ^b | EC number | Buffer for activity assay ^c | Q(standard buffer/enzyme-specific buffer) | Specific activity(current study/literature) in $\mu\text{mol}/(\text{min mg})^{\text{d}}$ |
|---|----------------------|-----------|--|---|---|
| 6-Phosphogluconolactonase | PF14_0511 | 3.1.1.31 | 25 mM Hepes and 2 mM MgCl_2 (pH 7.1)[9] | 1.0/1.0 | 145/10.2–60[8,25] |
| 6-Pyruvoyltetrahydropterin synthase | PFF1360w | 4.2.3.12 | 50 mM Tris, 100 mM KCl, 100 μM MgCl_2 , and 2 mM DTT (pH 8.0)[26] | 1.0/0.97 | >0/>0[26] |
| 6-Pyruvoyltetrahydropterin synthase(<i>P. vivax</i>) | PVX_114505 | 4.2.3.12 | 50 mM Tris, 100 mM KCl, 10 mM MgCl_2 , and 2 mM DTT (pH 8.0)[26] | 1.0/1.0 | >0/>0[26] |
| Adenosine deaminase | PF10_0289 | 3.5.4.4 | 20 mM potassium phosphate and 1 μM EDTA (pH 7.0)[27] | 0.05/0.15 | 11/>0[28] |
| Adenosine deaminase(<i>P. vivax</i>) | PVX_111245 | 3.5.4.4 | 20 mM potassium phosphate and 1 μM EDTA (pH 7.0)[27] | 0.63/0.75 | 100/>0[28] |
| Adenylosuccinate lyase(<i>P. vivax</i>) | PVX_114710 | 4.3.2.2 | 50 mM potassium phosphate (pH 7.4)[29] | 1.0/1.0 | 14/5.7–8.0[29] |
| Adenylosuccinate synthetase | PF13_0287 | 6.3.4.4 | 50 mM sodium phosphate and 5 mM MgCl_2 (pH 7.5)[30] | 1.0/1.0 | 0.9/1.14[30] |
| Aspartate carbamoyltransferase (<i>P. vivax</i>) | PVX_083135 | 2.1.3.2 | 50 mM Tris, 1 mM EDTA, 1 mM mercaptoethanol, and 400 fM BSA (pH 8.0)[31] | 0.92/1.0 | >0/NA |
| Choline kinase | PF14_0020 | 2.7.1.32 | 100 mM glycine–NaOH, 150 mM KCl, and 6 mM MgCl_2 (pH 9.2)[6] | 1.0/0.82 | 5/0.8[6] |
| D-Ribulose-5-phosphate 3-epimerase | PFL0960w | 5.1.3.1 | 300 mM triethanolamine (pH 7.4)[32] | 0.91/0.83 | 30/NA |
| Deoxyribose-phosphate aldolase (<i>P. yoelii</i>) | PY02252 | 4.1.2.4 | 100 mM triethanolamine (pH 7.5)[33] | 1.0/1.0 | 4.2/NA |
| Dihydrofolate synthase | PF13_0140 | 6.3.2.12 | 86 mM Tris, 100 mM KCl, and 4 mM MgCl_2 (pH 8.0)[34,35] | 0.05/0.06 | None/NA |
| dUTPase | PF11_0282 | 3.6.1.23 | 2.5 mM Mes, 100 mM KCl, 5 mM MgCl_2 , and 2.5 mM DTT (pH 6.2)[7] | 1.0/1.0 | 63/25.8[7] |
| Farnesyl pyrophosphate synthase (<i>P. vivax</i>) | PVX_092040 | 2.5.1.10 | 25 mM Hepes and 2.5 mM MgCl_2 (pH 7.4)[36] | 0.78/0.81 | 0.013/>0[36] |
| Glutamate dehydrogenase, NADP specific | PF14_0164 | 1.4.1.4 | 100 mM potassium phosphate and 1 mM EDTA (pH 8.0)[37] | 1.0/0.81 | 4.2/9[37] |
| Glyceraldehyde-3-phosphate dehydrogenase | PF14_0598 | 1.2.1.12 | 40 mM triethanolamine and 50 mM Na_2HPO_4 (pH 7.6)[38] | 1.0/1.0 | 23/90–120[38] |
| Glycerol-3-phosphate dehydrogenase | PFL0780w | 1.1.1.8 | 300 mM triethanolamine (pH 7.4)[39] | 1.0/1.0 | 6/NA |
| Guanylate kinase(<i>P. vivax</i>) | PVX_099895 | 2.7.4.8 | 50 mM Tris, 50 mM KCl, and 2 mM MgCl_2 (pH 7.5)[13] | 1.0/1.0 | 350/750[40] |
| Hydroxymethyldihydropterin pyrophosphokinase(<i>P. vivax</i>) | PVX_123230 | 2.7.6.3 | 100 mM Tris, 100 mM mercaptoethanol, and 10 mM MgCl_2 (pH 9.0)[41] | 0.44/0.18 | 0.01/0.01[41] |
| Methionine adenosyltransferase | PF11090w | 2.5.1.6 | 100 mM Tris, 150 mM KCl, 20 mM MgCl_2 , and 5 mM mercaptoethanol (pH 8.2)[42] | 0.44/0.49 | None/>0[42] |
| Methionine aminopeptidase 1 | PF10_0150 | 3.4.11.18 | 25 mM Hepes and 150 mM KCl (pH 7.5)[15] | 1.0/1.0 | 0.02*/0.23[14] |
| Methionine aminopeptidase 2 | PF14_0327 | 3.4.11.18 | 25 mM Hepes and 150 mM KCl (pH 7.5)[15] | 0.00/0.00 | None/0[23] |
| N-Myristoyltransferase | PF14_0127 | 2.3.1.97 | 20 mM Tris, 100 mM NaCl, and 1 mM EDTA (pH 8.0)[43] | 1.0/1.0 | 0.14*/> 0[44] |
| Nucleoside diphosphate kinase B | PF13_0349 | 2.7.4.6 | 50 mM Tris, 40 mM KCl, and 2 mM MgCl_2 (pH 7.2)[45] | 1.0/1.0 | 60*/1880[45] |
| Orotidine 5'-monophosphate decarboxylase | PF10_0225 | 4.1.1.23 | 25 mM Mops and 5% glycerol (pH 7.2)[46] | 1.0/1.0 | 11/2.7[46] |
| Phosphoethanolamine N-methyltransferase | MAL13P1.214 | 2.1.1.103 | 100 mM Hepes, 10% glycerol, and 2 mM EDTA (pH 8.6)[47] | 0.38/0.34 | 0.0001/0.0012[47] |
| Phosphoglycerate kinase | PF11105w | 2.7.2.3 | 100 mM triethanolamine, 5 mM MgSO_4 , 1 mM EDTA, and 1 mM DTT (pH 7.6)[48] | 1.0/1.0 | None/210[48] |
| Ribose 5-phosphate isomerase | PFE0730c | 5.3.1.6 | 300 mM triethanolamine (pH 7.4)[32] | 1.0/1.0 | 2100/NA |
| S-Adenosylhomocysteine hydrolase | PFE1050w | 3.3.1.1 | 25 mM potassium phosphate (pH 7.2)[49] | 0.45/0.47 | 0.028/0.03[49] |
| Superoxide dismutase(<i>P. berghei</i>) | PB000490.02.0 | 1.15.1.1 | 50 mM potassium phosphate, 0.1 mM EDTA (pH 7.8) [19] | 1.0/1.0 | 1400*/1631 [19] |
| Superoxide dismutase(<i>P. knowlesi</i>) | PKH_142350 | 1.15.1.1 | 50 mM potassium phosphate and 0.1 mM EDTA (pH 7.8)[19] | 1.0/1.0 | 1400*/1631[19] |

^a All enzymes are from *P. falciparum* unless otherwise noted.

^b Gene IDs are as assigned by PlasmoDB (<http://plasmodb.org>).

^c Activity assays were performed according to the references given. Exceptions and clarifications are noted in Materials and methods.

^d Literature values for specific activities are taken from previous studies of the same enzyme or an orthologue within the *Plasmodium* genus. Asterisks in the specific activity column indicate differences in assay substrates between previous studies and the current one (see Materials and methods). A specific activity of “NA” indicates that a literature value is not available. A value of “>0” means that the enzyme is active but the specific activity was not reported in the literature (and/or in the current study) and could not be determined because of a lack of calibration standards. Approximate assay detection limits for the enzymes with no detectable activity were 0.0002 $\mu\text{mol}/(\text{min mg})$ for dihydrofolate synthase, 0.003 $\mu\text{mol}/(\text{min mg})$ for methionine adenosyltransferase, 0.005 $\mu\text{mol}/(\text{min mg})$ for methionine aminopeptidase 2, and 0.0005 $\mu\text{mol}/(\text{min mg})$ for phosphoglycerate kinase.

and duration of preheating and concentrations of SDS) were empirically adjusted for each enzyme so that a wide range of activities and melting curve qualities could be observed within each dataset.

Heating was done at 58 °C for 0, 2, 5, 10, and 20 min with adenosine deaminase; 50 °C for 0, 2, 5, 10, and 20 min with glyceraldehyde-3-phosphate dehydrogenase; 50 °C for 0, 2, 10, and 20 min

with methionine aminopeptidase 1; and 61 °C for 1, 10, 20, and 40 min with orotidine 5'-monophosphate decarboxylase. SDS concentrations tested were 0%, 0.0125%, 0.02%, 0.03%, and 0.04% for adenosine deaminase; 0%, 0.01%, 0.0125%, 0.02%, and 0.03% for glyceraldehyde-3-phosphate dehydrogenase; 0%, 0.0156%, 0.031%, 0.0625%, and 0.125% for methionine aminopeptidase 1; and 0%, 0.01%, 0.02%, and 0.04% for orotidine 5'-monophosphate decarboxylase. Preassay denaturation of orotidine 5'-monophosphate decarboxylase was also attempted through repeated thawing/refreezing and with various concentrations of guanidine hydrochloride and urea.

Results

Melting curves were collected for 31 *Plasmodium* enzymes both in a standard buffer commonly used for thermal melt assays (100 mM Hepes and 150 mM KCl, pH 7.5) [3,20] and in each enzyme's activity assay buffer (listed in Table 1). There was a strong correlation ($R^2 = 0.945$) between an enzyme's Q (which quantifies melting curve quality (see Materials and methods)) in the standard buffer and its Q in activity assay buffer (Fig. 1).

Most enzymes' melting curves included a temperature span over which fluorescence increased substantially (presumably due to heat-induced unfolding), resulting in Q values above 0.60. Of these 24 high- Q enzymes, 23 were catalytically active (Fig. 2). Fluorescence increases due to melting were small for seven enzymes, leading to Q values below 0.50. Among these seven, only four were found to be active (Fig. 2). Another way of summarizing these results is to say that, of the four inactive enzymes, all but one had Q values below 0.50. These data suggest that a good melting curve, as indicated by a high Q , is predictive of catalytic activity.

As a further exploration of the relationship between melting curve quality and enzyme activity, we studied how both change in response to varying degrees of preassay denaturation. Preliminary experiments gauged the response of orotidine 5'-monophosphate decarboxylase to five possible causes of denaturation: prolonged heating, repeated thawing/refreezing, exposure to SDS, exposure to guanidine hydrochloride, and exposure to urea. Repeated freezing/thawing (5–10 cycles) and exposure to urea (≤ 1.8 M) did not cause significant changes in enzyme behavior,

and guanidine hydrochloride was found to be a competitive inhibitor of the enzyme at subdenaturing concentrations (data not shown). However, preheating and SDS were found to denature the enzyme effectively and unambiguously, so these perturbations were then used to study three additional *Plasmodium* enzymes: adenosine deaminase (from *P. vivax*), glyceraldehyde-3-phosphate dehydrogenase, and methionine aminopeptidase 1. Typical changes in melting curves in response to preheating and SDS are shown in Fig. 3. As the [SDS] or duration of preheating increased, the initial fluorescence (at 20 °C) increased and the change in fluorescence associated with melting (ΔF_{melt}) decreased. The melting temperature (T_m), defined as the temperature at which the fluorescence increases most steeply [3], decreased in response to SDS but not in response to preheating. These trends were similar for all four enzymes.

Fig. 4 shows the relationships between Q values and activities of the four enzymes denatured with preheating and with SDS. A full range of conditions was employed, up to and including those producing activities at or near 0%. It is evident that in many instances, a treated enzyme can suffer substantial deterioration of its melting curves, as indicated by Q values at or near 0, but still retain significant activity. The denaturation of adenosine deaminase by SDS is the clearest example of this somewhat surprising trend. Nevertheless, the general pattern suggested by Fig. 2 also applies here: high- Q samples were quite active, whereas the activities of low- Q samples were harder to predict.

Two limitations of the data presented so far are that (i) only *Plasmodium* enzymes were studied and (ii) the denaturation of enzymes as explored in Figs. 3 and 4 was achieved artificially (i.e., with conditions to which valuable proteins are unlikely to be subjected). Can Q values be used to predict whether enzymes from any organism are active even when normal measures are taken to preserve their functional three-dimensional shape? As a preliminary look at this question, we studied pairs of stocks of xanthine oxidase from *B. taurus* (purchased from Sigma–Aldrich) and cysteine protease 1 from *E. histolytica* (expressed in *E. coli* by our lab). Both stocks of xanthine oxidase had been stored at 4 °C as recommended by the manufacturer, but at the time of these experiments one stock was 14 months old and the other was only 4 months old. The melting curve of the older stock did not show a melting-related increase in fluorescence ($Q = 0.00$), whereas the newer stock

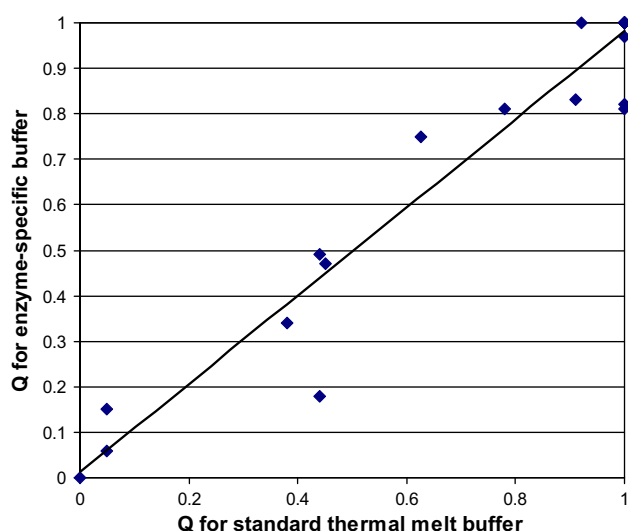


Fig. 1. Melting curve quality is similar in standard and enzyme-specific buffers. Q values were calculated as described in Materials and methods. Each score is an average of 5–8 replicate wells. Each data point represents a separate *Plasmodium* enzyme; many enzymes are represented by the point at (1, 1). The best fit line is $y = 0.97x + 0.01$ ($R^2 = 0.94$).

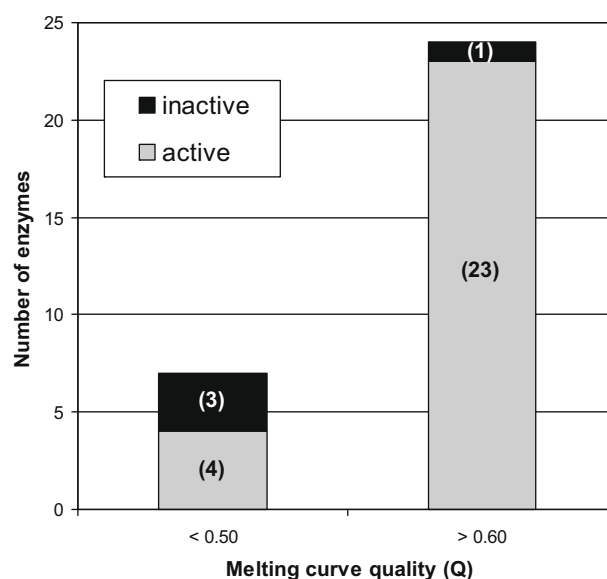


Fig. 2. *Plasmodium* enzymes with high Q values (> 0.60) are almost always active, whereas those with lower Q values (< 0.50) are more variable.

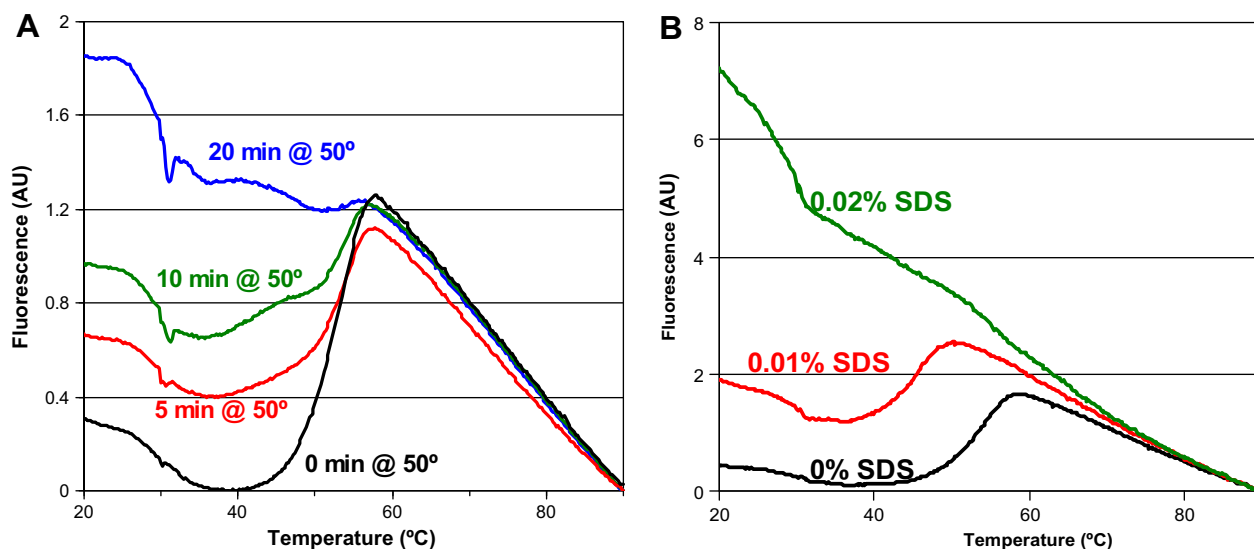


Fig. 3. Melting curves for glyceraldehyde-3-phosphate dehydrogenase in activity assay buffer in response to preheating (A) and SDS (B). Data shown are typical results from single wells. AU, arbitrary units.

showed a small but distinct increase between 60 and 70 °C ($Q = 0.05$) (Fig. 5A). When both stocks were tested for catalytic activity, only the newer stock was found to be active (with a specific activity of 0.04 $\mu\text{mol}/(\text{min mg})$; detection limit $\sim 0.004 \mu\text{mol}/(\text{min mg})$). Similar assays were performed with two stocks of cysteine protease 1, one of which had been refolded with buffers optimized for this particular enzyme. The stock to which optimal refolding buffers had been applied gave a melting curve with a middling Q (0.40) and was active, whereas the other stock had a low Q (0.10) (Fig. 5B) and was not active (detection limit not known).

Discussion

This article has presented evidence that enzymes with high-quality thermal melt curves, as indicated by high Q values, are more likely to be catalytically active than enzymes with poor melting curves. The relationship between melting curves and activity was examined in three sets of enzymes: 31 recombinant *Plasmodium* enzymes expressed and purified with standard protocols (Fig. 2), a subset of four *Plasmodium* enzymes artificially denatured with heat and SDS (Figs. 3 and 4), and two pairs of non-*Plasmodium* enzymes (Fig. 5). These datasets collectively indicate that the higher the Q of an enzyme stock, the more likely it is to be active. The implication is that melting curves are a reasonable indicator of whether a protein is denatured or natively folded and that thermal melt assays could be used to assess the folding status of noncatalytic proteins as well as enzymes.

Our conclusion that melting curves indicate protein folding status comes with at least four caveats. First, our study focused entirely on enzymes (rather than noncatalytic proteins) and mainly on *Plasmodium* enzymes, whose amino acid composition differs from that of most organisms due to the AT richness of the *Plasmodium* genome [21]. Second, melting curves reveal only whether hydrophobic residues are exposed to surrounding solvent and, thus, cannot distinguish between proteins that are properly folded and proteins that are misfolded in a way that nonetheless shields their hydrophobic regions from solvent. The inactivity of our stock of phosphoglycerate kinase could, in theory, be due to this type of misfolding. Third, an enzyme's overall three-dimensional structure is only one of several determinants of its activity; for instance, the absence of a cofactor or point mutations in the active site might

not significantly alter an enzyme's gross structure but may render it inactive. As an example, a methionine aminopeptidase 1 stock purified with cobalt rather than manganese gave good melting curves ($Q = 1$) but was inactive unless manganese, its probable cofactor in vivo [22], was added to the assay buffer (data not shown). Fourth, we did not prove that $\Delta F_{\text{melt}}/\Delta F_{\text{total}}$ (the ratio of the melting-associated rise in fluorescence to the total range of fluorescence values observed between 20 and 90 °C) is the best possible measure of melting curve quality. Data such as those in Fig. 3 show that as an enzyme becomes more and more denatured, its ΔF_{melt} tends to decrease, whereas its initial fluorescence at 20 °C (and usually ΔF_{total}) tends to increase. Calculating Q as the ratio of ΔF_{melt} to ΔF_{total} is a simple and logical way of capturing both trends; however, alternative metrics for rating melting curves may be equally appropriate, depending on the goals of one's analysis.

In measuring specific activities of our *Plasmodium* enzymes, we followed precedents reported in the literature whenever possible so that our values could be compared with previously reported values. These comparisons (Table 1) did not reveal any obvious patterns; for example, low- Q enzymes did not consistently have specific activities well below literature values. This might not be surprising because, aside from possible lab-to-lab differences in assay performance, we do not know how other labs' enzyme stocks compare with ours in terms of purity and folding state. If a recombinant enzyme expressed in *E. coli* tends to misfold under standard expression and purification conditions, it might have a low or non-existent specific activity both in our lab and elsewhere. Indeed, our failure to detect activity of recombinant methionine aminopeptidase 2 from *P. falciparum* is consistent with a previous report [23].

The current study helps to clarify previous speculation in the literature regarding melting curves having a high baseline fluorescence and/or lacking a large melting-related increase in fluorescence. It has been proposed that high initial fluorescence is "likely caused by the dye binding to hydrophobic parts of the protein that are exposed even when it is fully folded" and that the lack of a melting transition "can be explained by high protein T_m that exceed the maximum temperature limit of the instruments" [24]. If poor melting curves usually come from properly folded proteins, as implied by the preceding sentence, melting curve quality would not be a useful indicator of an enzyme's folding status and would not correlate with catalytic activity. On the contrary, our results

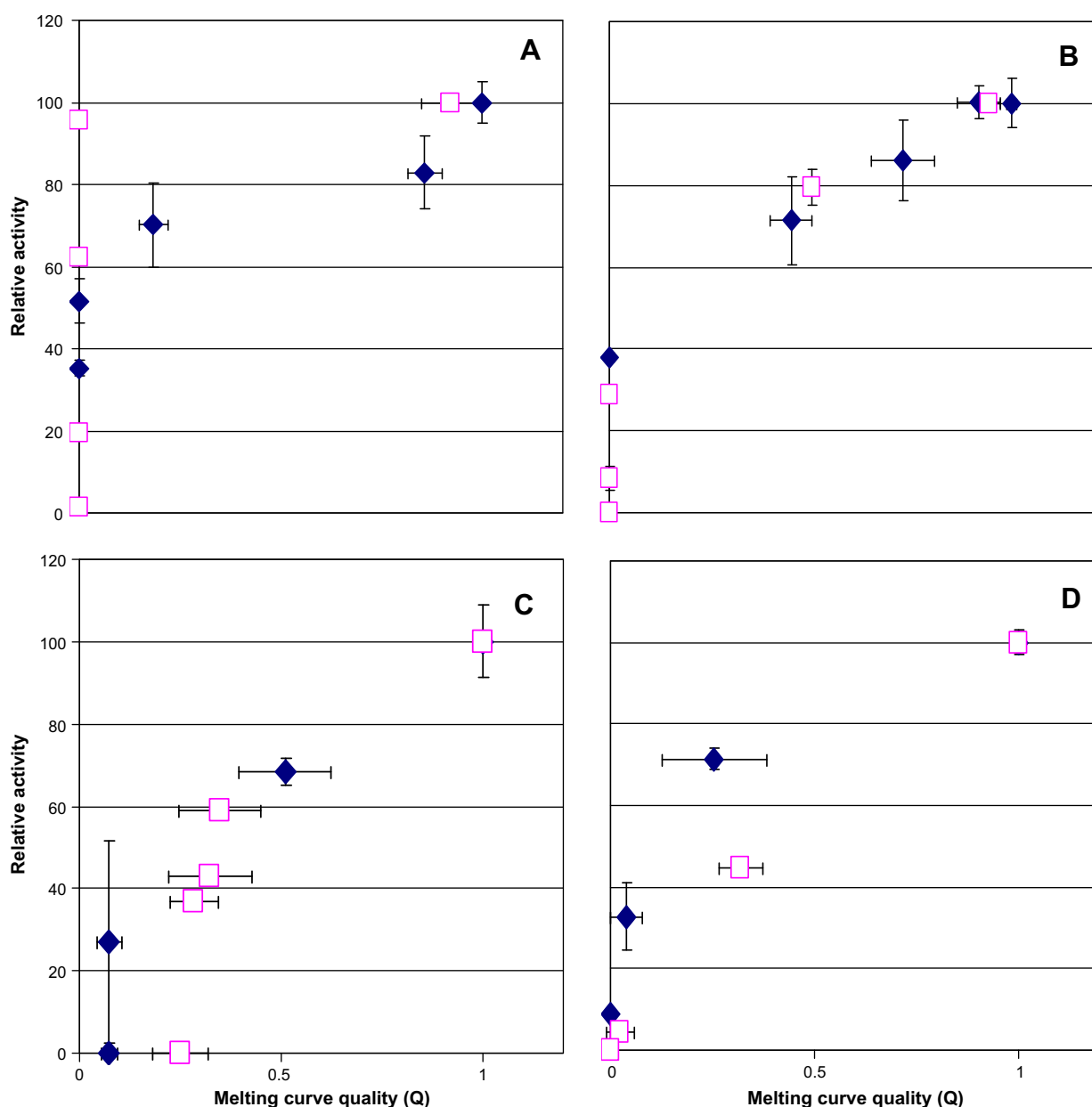


Fig. 4. Q values and activities for adenosine deaminase (A), glyceraldehyde-3-phosphate dehydrogenase (B), methionine aminopeptidase 1 (C), and orotidine 5'-monophosphate decarboxylase (D) denatured by heat (solid diamonds) and SDS (open squares). Error bars represent standard deviations.

show that enzymes with poor melting curves are less likely to be active, suggesting that a poor melting curve is often a result of being poorly folded. However, it is possible that well-folded stocks of certain proteins yield poor melting curves for the reasons offered above, and these reasons may account for the relatively high activities of some of our low-Q enzymes.

Thermal melt curves have previously been shown to be useful for optimizing protein purification, concentration, and crystallization, with the optimal conditions being those in which the protein's T_m is maximized [20]. Members of our research group have also found that melting curves help to predict whether proteins can be crystallized (F. Zucker et al., unpublished experiments). The current study supports and extends those findings by demonstrating that melting curve quality is predictive of enzyme activity and, therefore, appears to be a reasonable indicator of folding status. These new results, in turn, hint that thermal melt assays may have additional applications beyond their use in crystallography.

For example, a lab that has purified many proteins may wish to prioritize a few of them in developing functional assays for high-throughput screening. Because the functional assays may be difficult and costly to set up, thermal melt assays can be used to identify which proteins are most likely to be well-folded and, thus, which should be pursued further if resources are limited. (Such assays can probably be conducted with a single common buffer given that generic and enzyme-specific buffers yield similar results (Fig. 1).) Similarly, if a lab has generated many different stocks of the same protein, thermal melt assays may allow rapid assessment of the stocks without the need for functional assays. Finally, if a newly discovered protein appears to be inactive in an assay of its hypothesized function, thermal melting may help to establish whether the apparent inactivity is due to denaturation. If the protein's melting curves suggest that it is well-folded, the possibility that the protein's true function is not what was hypothesized should be considered.

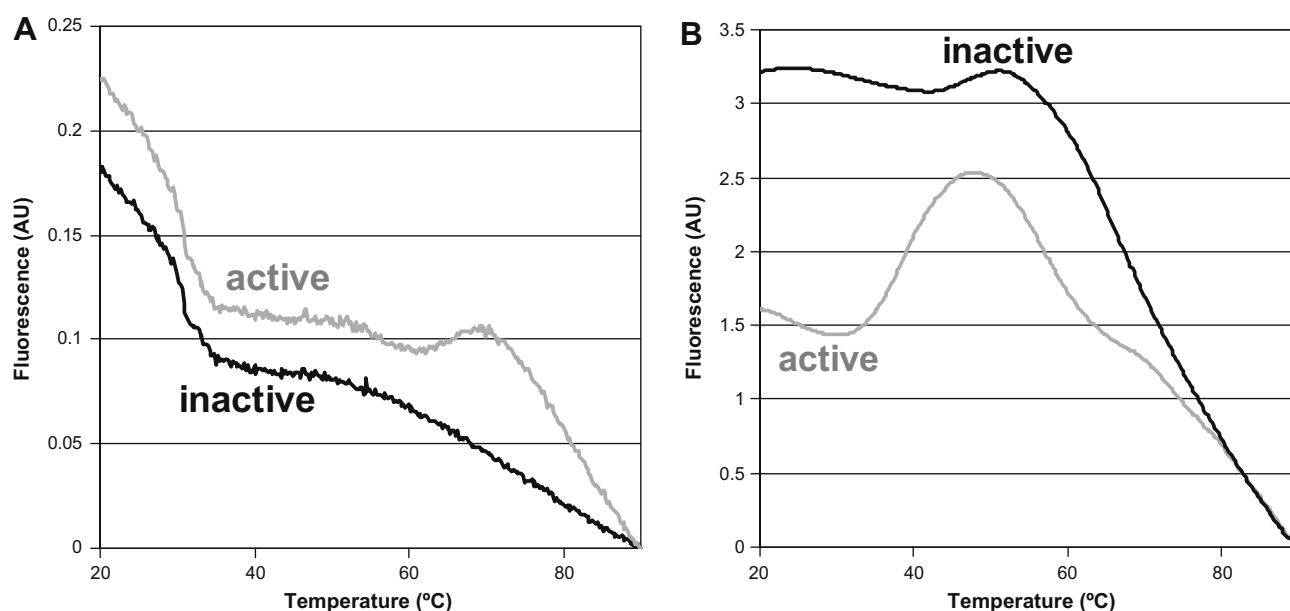


Fig. 5. Thermal melt curves of catalytically active and inactive stocks of xanthine oxidase from *B. taurus* (A) and cysteine protease 1 from *E. histolytica* (B). Data shown are typical results from single wells. AU, arbitrary units.

The preceding paragraphs should not be taken to mean that thermal melting is the only method conducive to high-throughput assessment of protein folding. The related technique of isothermal denaturation (ITD) also permits scanning of protein samples in 96- or 384-well plates, as does differential static light scattering (DSLS) [24], so those methods may also prove to be predictive of catalytic activity. The sample and time requirements of the three techniques are similar in that 5–25 μ l of protein at a concentration of 50–200 μ g/ml is needed for each well and scanning takes approximately 60 min. All three methods are distinct from circular dichroism (CD), another popular way of assessing protein folding, in that the latter requires a CD spectrometer (and therefore greater quantities of protein) and cannot be conducted in a high-throughput manner with commercially available plate readers. However, CD does offer the advantage of being nondestructive to protein samples.

Acknowledgments

Funding for this study was provided by the Medicines for Malaria Venture (MMV), the Medical Structural Genomics for Pathogenic Protozoa (MSGPP) program project, the National Institutes of Health (NIH) (AI067921 to W.G.J.H., AI080625 to W.C.V.V., AI077822-01 to Sharon L. Reed), and the United Nations Development Program (UNDP)/World Bank/World Health Organization (WHO) Special Program for Research and Training in Tropical Diseases (05-00508). We thank Raymond Hui of the University of Toronto's Structural Genomics Consortium for supplying plasmids for expressing four of the *Plasmodium* proteins used in this study. We also thank our University of Washington colleagues Erkang Fan, Zhongsheng Zhang, and Frank Zucker for insights on thermal melt assays and analysis, Frederick Buckner for target selection expertise, and Christophe Verlinde for comments on the manuscript.

References

- [1] M.W. Pantoliano, E.C. Petrella, J.D. Kwasnoski, V.S. Lobanov, J. Myslik, E. Graf, T. Carver, E. Asel, B.A. Springer, P. Lane, F.R. Salemme, High-density miniaturized thermal shift assays as a general strategy for drug discovery, *J. Biomol. Screen.* 6 (2001) 429–440.
- [2] T.M. Mezzasalma, J.K. Kranz, W. Chan, G.T. Struble, C. Schalk-Hihi, I.C. Deckman, B.A. Springer, M.J. Todd, Enhancing recombinant protein quality and yield by protein stability profiling, *J. Biomol. Screen.* 12 (2007) 418–428.
- [3] G.J. Crowther, A.J. Napuli, A.P. Thomas, D.J. Chung, K.V. Kovzun, D.J. Leibly, L.J. Castaneda, J. Bhandari, C.J. Damman, R. Hui, W.G.J. Hol, F.S. Buckner, C.L.M.J. Verlinde, Z. Zhang, E. Fan, W.C. Van Voorhis, Buffer optimization of thermal melt assays of *Plasmodium* proteins for detection of small-molecule ligands, *J. Biomol. Screen.* 14 (2009) 700–707.
- [4] A. Bracher, W. Eisenreich, N. Schramek, H. Ritz, E. Gotze, A. Herrmann, M. Gutlich, A. Bacher, Biosynthesis of pteridines: NMR studies on the reaction mechanisms of GTP cyclohydrolase I, pyruvoyltetrahydropterin synthase, and sepiapterin reductase, *J. Biol. Chem.* 273 (1998) 28132–28141.
- [5] S.G. Melendez-Lopez, S. Herdman, K. Hirata, M.H. Choi, Y. Choe, C. Craik, C.R. Caffrey, E. Hansell, B. Chavez-Munguia, Y.T. Chen, W.R. Roush, J. McKerrow, L. Eckmann, J. Guo, S.L. Stanley Jr., S.L. Reed, Use of recombinant *Entamoeba histolytica* cysteine proteinase 1 to identify a potent inhibitor of amebic invasion in a human colonic model, *Eukaryot. Cell* 6 (2007) 1130–1136.
- [6] V. Choubey, M. Guha, P. Maity, S. Kumar, R. Raghunandan, P.R. Maulik, K. Mitra, U.C. Halder, U. Bandyopadhyay, Molecular characterization and localization of *Plasmodium falciparum* choline kinase, *Biochim. Biophys. Acta* 1760 (2006) 1027–1038.
- [7] J.L. Whittingham, I. Leal, C. Nguyen, G. Kasinathan, E. Bell, A.F. Jones, C. Berry, A. Benito, J.P. Turkenburg, E.J. Dodson, L.M. Ruiz Perez, A.J. Wilkinson, N.G. Johansson, R. Brun, I.H. Gilbert, D. Gonzalez Pacanowska, K.S. Wilson, dUTPase as a platform for antimalarial drug design: structural basis for the selectivity of a class of nucleoside inhibitors, *Structure* 13 (2005) 329–338.
- [8] J.L. Clarke, D.A. Scopes, O. Sodeinde, P.J. Mason, Glucose-6-phosphate dehydrogenase-6-phosphogluconolactonase: a novel bifunctional enzyme in malaria parasites, *Eur. J. Biochem.* 268 (2001) 2013–2019.
- [9] F. Collard, J.F. Collet, I. Gerin, M. Veiga-da-Cunha, E. Van Schaftingen, Identification of the cDNA encoding human 6-phosphogluconolactonase, the enzyme catalyzing the second step of the pentose phosphate pathway (1), *FEBS Lett.* 459 (1999) 223–226.
- [10] M. Koresawa, T. Okabe, High-throughput screening with quantitation of ATP consumption: a universal non-radioisotope, homogeneous assay for protein kinase, *Assay Drug Dev. Technol.* 2 (2004) 153–160.
- [11] X. Que, L.S. Brinen, P. Perkins, S. Herdman, K. Hirata, B.E. Torian, H. Rubin, J.H. McKerrow, S.L. Reed, Cysteine proteinases from distinct cellular compartments are recruited to phagocytic vesicles by *Entamoeba histolytica*, *Mol. Biochem. Parasitol.* 119 (2002) 23–32.
- [12] P.P. Van Veldhoven, G.P. Mannaerts, Inorganic and organic phosphate measurements in the nanomolar range, *Anal. Biochem.* 161 (1987) 45–48.
- [13] Sigma-Aldrich, Enzymatic assay of guanylate kinase (EC 2.7.4.8), 2009. Available from: <http://www.sigmaaldrich.com/etc/medialib/docs/Sigma/Enzyme_Assay/guanylatekinase.Par.0001.File.tmp/guanylatekinase.pdf>.
- [14] X. Chen, C.R. Chong, L. Shi, T. Yoshimoto, D.J. Sullivan Jr., J.O. Liu, Inhibitors of *Plasmodium falciparum* methionine aminopeptidase 1b possess antimalarial activity, *Proc. Natl. Acad. Sci. USA* 103 (2006) 14548–14553.
- [15] S. Mitra, A.M. Dygas-Holz, J. Jiracek, M. Zertova, L. Zakova, R.C. Holz, A new colorimetric assay for methionyl aminopeptidases: examination of the binding of a new class of pseudopeptide analog inhibitors, *Anal. Biochem.* 357 (2006) 43–49.

- [16] S. Rahlfs, S. Koncarevic, R. Iozef, B.M. Mailu, S.N. Savvides, R.H. Schirmer, K. Becker, Myristoylated adenylate kinase-2 of *Plasmodium falciparum* forms a heterodimer with myristoyltransferase, *Mol. Biochem. Parasitol.* 163 (2009) 77–84.
- [17] S.K. Wright, R.E. Viola, Evaluation of methods for the quantitation of cysteines in proteins, *Anal. Biochem.* 265 (1998) 8–14.
- [18] S. Gratepanche, S. Menage, D. Touati, R. Wintjens, P. Delplace, M. Fontecave, A. Masset, D. Camus, D. Dive, Biochemical and electron paramagnetic resonance study of the iron superoxide dismutase from *Plasmodium falciparum*, *Mol. Biochem. Parasitol.* 120 (2002) 237–246.
- [19] Sigma–Aldrich, Enzymatic assay of superoxide dismutase (1.15.1.1), 2009. Available from: <http://www.sigmaaldrich.com/etc/medialib/docs/Sigma/General_Information/superoxide_dismutase.Par.0001.File.tmp/superoxide_dismutase.pdf>.
- [20] M. Vedadi, F.H. Niesen, A. Allali-Hassani, O.Y. Fedorov, P.J. Finerty Jr., G.A. Wasney, R. Yeung, C. Arrowsmith, L.J. Ball, H. Berglund, R. Hui, B.D. Marsden, P. Nordlund, M. Sundstrom, J. Weigelt, A.M. Edwards, Chemical screening methods to identify ligands that promote protein stability, protein crystallization, and structure determination, *Proc. Natl. Acad. Sci. USA* 103 (2006) 15835–15840.
- [21] O. Bastien, S. Lespinats, S. Roy, K. Metayer, B. Fertil, J.J. Codani, E. Marechal, Analysis of the compositional biases in *Plasmodium falciparum* genome and proteome using *Arabidopsis thaliana* as a reference, *Gene* 336 (2004) 163–173.
- [22] J. Wang, G.S. Sheppard, P. Lou, M. Kawai, C. Park, D.A. Egan, A. Schneider, J. Bouska, R. Lesniewski, J. Henkin, Physiologically relevant metal cofactor for methionine aminopeptidase-2 is manganese, *Biochemistry* 42 (2003) 5035–5042.
- [23] X. Chen, S. Xie, S. Bhat, N. Kumar, T.A. Shapiro, J.O. Liu, Fumagillin and fumarranol interact with *P. falciparum* methionine aminopeptidase 2 and inhibit malaria parasite growth in vitro and in vivo, *Chem. Biol.* 16 (2009) 193–202.
- [24] G.A. Senisterra, P.J. Finerty Jr., High throughput methods of assessing protein stability and aggregation, *Mol. Biosyst.* 5 (2009) 217–223.
- [25] E. Miclet, V. Stoven, P.A. Michels, F.R. Oppendoes, J.Y. Lallemand, F. Duffieux, NMR spectroscopic analysis of the first two steps of the pentose–phosphate pathway elucidates the role of 6-phosphogluconolactonase, *J. Biol. Chem.* 276 (2001) 34840–34846.
- [26] S. Ditttrich, S.L. Mitchell, A.M. Blagborough, Q. Wang, P. Wang, P.F. Sims, J.E. Hyde, An atypical orthologue of 6-pyruvoyltetrahydropterin synthase can provide the missing link in the folate biosynthesis pathway of malaria parasites, *Mol. Microbiol.* 67 (2008) 609–618.
- [27] P.C. Tyler, E.A. Taylor, R.F. Frohlich, V.L. Schramm, Synthesis of 5'-methylthio cofamylcins: specific inhibitors for malarial adenosine deaminase, *J. Am. Chem. Soc.* 129 (2007) 6872–6879.
- [28] P.E. Daddona, W.P. Wiesmann, C. Lambros, W.N. Kelley, H.K. Webster, Human malaria parasite adenosine deaminase: characterization in host enzyme-deficient erythrocyte culture, *J. Biol. Chem.* 259 (1984) 1472–1475.
- [29] V. Bulusu, B. Srinivasan, M.P. Bopanna, H. Balaram, Elucidation of the substrate specificity, kinetic, and catalytic mechanism of adenylosuccinate lyase from *Plasmodium falciparum*, *Biochim. Biophys. Acta* 1794 (2009) 642–654.
- [30] R. Jayalakshmi, K. Sumathy, H. Balaram, Purification and characterization of recombinant *Plasmodium falciparum* adenylosuccinate synthetase expressed in *Escherichia coli*, *Protein Expr. Purif.* 25 (2002) 65–72.
- [31] A.J. Else, G. Herve, A microtiter plate assay for aspartate transcarbamylase, *Anal. Biochem.* 186 (1990) 219–221.
- [32] T. Wood, Spectrophotometric assay for D-ribose-5-phosphate ketol isomerase and D-ribulose-5-phosphate 3-epimerase, *Anal. Biochem.* 33 (1970) 297–306.
- [33] H. Sakuraba, K. Yoneda, K. Yoshihara, K. Satoh, R. Kawakami, Y. Uto, H. Tsuge, K. Takahashi, H. Hori, T. Ohshima, Sequential aldol condensation catalyzed by hyperthermophilic 2-deoxy-D-ribose-5-phosphate aldolase, *Appl. Environ. Microbiol.* 73 (2007) 7427–7434.
- [34] I. Levin, M. Mevarech, B.A. Palffy, Characterization of a novel bifunctional dihydropteroate synthase/dihydropteroate reductase enzyme from *Helicobacter pylori*, *J. Bacteriol.* 189 (2007) 4062–4069.
- [35] A.L. Bognar, C. Osborne, B. Shane, S.C. Singer, R. Ferone, Folylpolypoly-γ-glutamate synthetase–dihydrofolate synthetase: cloning and high expression of the *Escherichia coli folC* gene and purification and properties of the gene product, *J. Biol. Chem.* 260 (1985) 5625–5630.
- [36] D. Mukkamala, J.H. No, L.M. Cass, T.K. Chang, E. Oldfield, Bisphosphonate inhibition of a *Plasmodium farnesyl* diphosphate synthase and a general method for predicting cell-based activity from enzyme data, *J. Med. Chem.* 51 (2008) 7827–7833.
- [37] J.T. Wagner, H. Ludemann, P.M. Farber, F. Lottspeich, R.L. Krauth-Siegel, Glutamate dehydrogenase, the marker protein of *Plasmodium falciparum*: cloning, expression, and characterization of the malarial enzyme, *Eur. J. Biochem.* 258 (1998) 813–819.
- [38] N. Campanale, C. Nickel, C.A. Daubenberger, D.A. Wehlan, J.J. Gorman, N. Klonis, K. Becker, L. Tilley, Identification and characterization of heme-interacting proteins in the malaria parasite, *Plasmodium falciparum*, *J. Biol. Chem.* 278 (2003) 27354–27361.
- [39] Sigma–Aldrich, Enzymatic assay of α-glycerophosphate dehydrogenase (EC 1.1.1.8), 2009. Available from: <http://www.sigmaaldrich.com/etc/medialib/docs/Sigma/Enzyme_Assay/aglycerophosdehydro.Par.0001.File.dat/aglycerophosdehydro.pdf>.
- [40] M. Kandeel, M. Nakanishi, T. Ando, K. El-Shazly, T. Yosef, Y. Ueno, Y. Kitade, Molecular cloning, expression, characterization, and mutation of *Plasmodium falciparum* guanylate kinase, *Mol. Biochem. Parasitol.* 159 (2008) 130–133.
- [41] W. Kasekarn, R. Sirawaraporn, T. Chahomchuen, A.F. Cowman, W. Sirawaraporn, Molecular characterization of bifunctional hydroxymethyl-dihydropterin pyrophosphokinase–dihydropteroate synthase from *Plasmodium falciparum*, *Mol. Biochem. Parasitol.* 137 (2004) 43–53.
- [42] P.K. Chiang, M.E. Chamberlin, D. Nicholson, S. Soubes, X. Su, G. Subramanian, D.E. Lanar, S.T. Prigge, J.P. Scovill, L.H. Miller, J.Y. Chou, Molecular characterization of *Plasmodium falciparum* S-adenosylmethionine synthetase, *Biochem. J.* 344 (1999) 571–576.
- [43] D.A. Towler, S.P. Adams, S.R. Eubanks, D.S. Towery, E. Jackson-Machelski, L. Glaser, J.I. Gordon, Purification and characterization of yeast myristoyl CoA:protein N-myristoyltransferase, *Proc. Natl. Acad. Sci. USA* 84 (1987) 2708–2712.
- [44] P.W. Bowyer, R.S. Gunaratne, M. Grainger, C. Withers-Martinez, S.R. Wickramasinghe, E.W. Tate, R.J. Leatherbarrow, K.A. Brown, A.A. Holder, D.F. Smith, Molecules incorporating a benzothiazole core scaffold inhibit the N-myristoyltransferase of *Plasmodium falciparum*, *Biochem. J.* 408 (2007) 173–180.
- [45] M. Kandeel, T. Miyamoto, Y. Kitade, Bioinformatics, enzymologic properties, and comprehensive tracking of *Plasmodium falciparum* nucleoside diphosphate kinase, *Biol. Pharm. Bull.* 32 (2009) 1321–1327.
- [46] D.B. Langley, M. Shojaei, C. Chan, H.C. Lok, J.P. Mackay, T.W. Traut, J.M. Guss, R.I. Christopherson, Structure and inhibition of orotidine 5'-monophosphate decarboxylase from *Plasmodium falciparum*, *Biochemistry* 47 (2008) 3842–3854.
- [47] G. Pessi, G. Kociubinski, C.B. Mamoun, A pathway for phosphatidylcholine biosynthesis in *Plasmodium falciparum* involving phosphoethanolamine methylation, *Proc. Natl. Acad. Sci. USA* 101 (2004) 6206–6211.
- [48] B. Pal, B. Pybus, D.D. Muccio, D. Chattopadhyay, Biochemical characterization and crystallization of recombinant 3-phosphoglycerate kinase of *Plasmodium falciparum*, *Biochim. Biophys. Acta* 1699 (2004) 277–280.
- [49] M. Nakanishi, A. Iwata, C. Yatome, Y. Kitade, Purification and properties of recombinant *Plasmodium falciparum* S-adenosyl-L-homocysteine hydrolase, *J. Biochem.* 129 (2001) 101–105.